ISOLATED STAR FORMATION IN BOK GLOBULES

R. LAUNHARDT

Max Planck Institute for Astronomy, Königstuhl 17, 69117 Heidelberg, Germany

Because of their isolated location and simple structure, the dense cores of nearby Bok globules are ideal laboratories to study in detail the process of low-mass star formation. In this paper we describe the general characteristics of Bok globules and summarize our current knowledge of the properties of their star-forming cores. In particular we discuss radial density profiles, evolutionary effects, multiplicity, magnetic fields, kinematic properties like rotation and turbulence, star-formation efficiency, and the overall energy balance.

Keywords: Stars: formation – ISM: clouds – ISM: magnetic fields

1 Introduction

Different aspects of star formation can be studied on different size scales and in different environments. The large-scale distribution of star-forming regions and the relation between molecular cloud life cycles, galactic spiral density waves, and star formation can be studied by observing nearby galaxies. The stellar initial mass function, which is needed to interpret these data, is usually derived from rich young stellar clusters in our own Galaxy. Dense star-forming dark cloud complexes like, e.g., the ρ Oph cloud are the places to study the relation between molecular clump mass spectra, turbulence, and star-formation. And finally, nearby isolated Bok globules are the best places to study in detail the initial properties of individual star-forming cores, their chemical evolution, kinematic structure, and the physics of collapse and fragmentation. However, one has to keep in mind that some of the results may be typical only for the isolated mode of star formation and may not be applicable to dense and clustered star-forming regions.

Bok globules are small, simply-structured, relatively isolated molecular clouds that often contain only one single star-forming core (e.g. Clemens & Barvainis 1988; Bourke et al. 1995). Figure 1 shows optical/NIR images of three "typical" nearby Bok globules together with contours of the thermal submm/mm dust emission from the dense star-forming cores. Table 1 summarizes the average general properties of typical Bok globules and their star-forming cores.

Although they are the most simple star-forming molecular clouds, most globules deviate considerably from spherical geometry. They are often cometary or irregularly shaped. The dense star-forming cores are often not located at the center of the globule, but in cometary-shaped globules located closer to the sharper rim ("head" side). Pre-protostellar cores often appear to be fragmentary and filamentary. However, the protostellar cores and envelopes of Class I YSOs are more spherically symmetric, which can be understood as a result of the gravitational collapse of the inner dense $R \sim 5000\,\mathrm{AU}$ region.

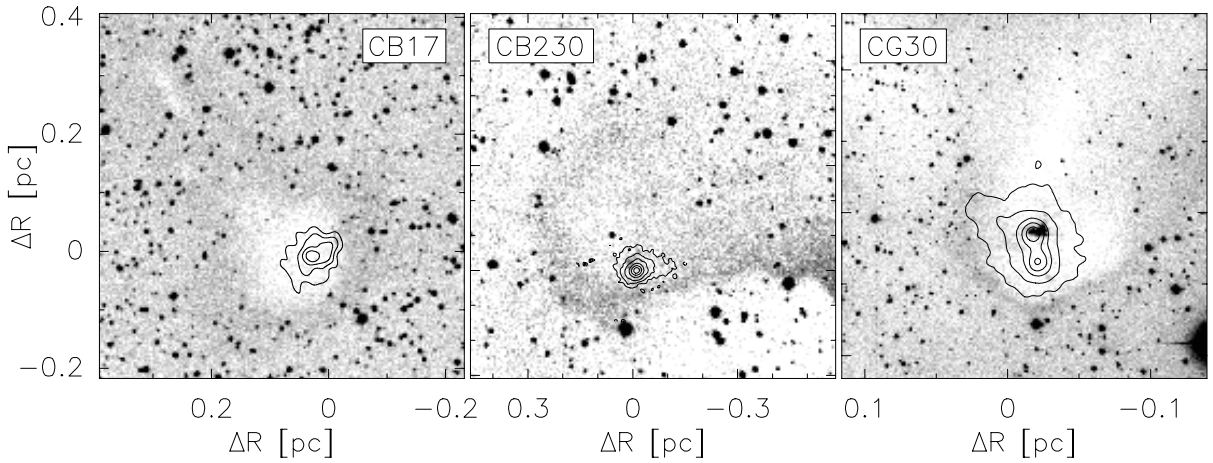

Figure 1: Optical/NIR images of "typical" nearby Bok globules ($D = 200 \ldots 400\,\mathrm{pc}$). Contours of the thermal mm dust emission mark the dense star-forming cores. Axis labeling in pc refers to the distance of the globules.

Table 1: Average general properties of Bok globules and their dense cores.

	Globule	Dense core
Mass	5 - 50 $\mathrm{M}_\odot$	1 - 5 $\mathrm{M}_\odot$
Radius	0.1 – 1 pc	~ 0.05 pc (10,000 AU)
Density	($10^3\,\mathrm{cm}^{-3}$)	$10^6\,\mathrm{cm}^{-3}$
Temperature	(15 K)	10 K
Line widths	$0.5 - 2\,\mathrm{km\,s}^{-1}$	$0.4 - 0.7\,\mathrm{km\,s}^{-1}$

2 Properties of the star-forming cores

2.1 Pre-protostellar cores

Based on submillimeter and millimeter dust continuum maps, models of isolated pre-protostellar cores in Taurus and in Bok globules have been derived by a number of authors (e.g., Ward-Thompson et al. 1994, 1999:, Evans et al. 2001; Launhardt et al. in prep.). Despite different modeling approaches, all authors derive some common features. Isolated pre-protostellar cores appear to have an inner flat-density core of radius few hundred to few thousand AU and central densities of one to a few $10^6\,\mathrm{cm}^{-3}$, an outer radial density profile that approaches $n_\mathrm{H} \propto R^{-2}$, a well-defined outer cut-off radius at $\sim 2 \times 10^4\,\mathrm{AU}$, and total mass between 2 and $5\,\mathrm{M}_\odot$. Typical masses inside $R < 5000\,\mathrm{AU}$ are of order $0.5 - 1\,\mathrm{M}_\odot$, i.e., $\sim$20% of the total core mass. Typical dust temperatures are $6 - 10\,\mathrm{K}$ in the inner core and $10 - 15\,\mathrm{K}$ towards the outer edge, which is due to external heating by the interstellar radiation field (e.g., Evans et al. 2001).

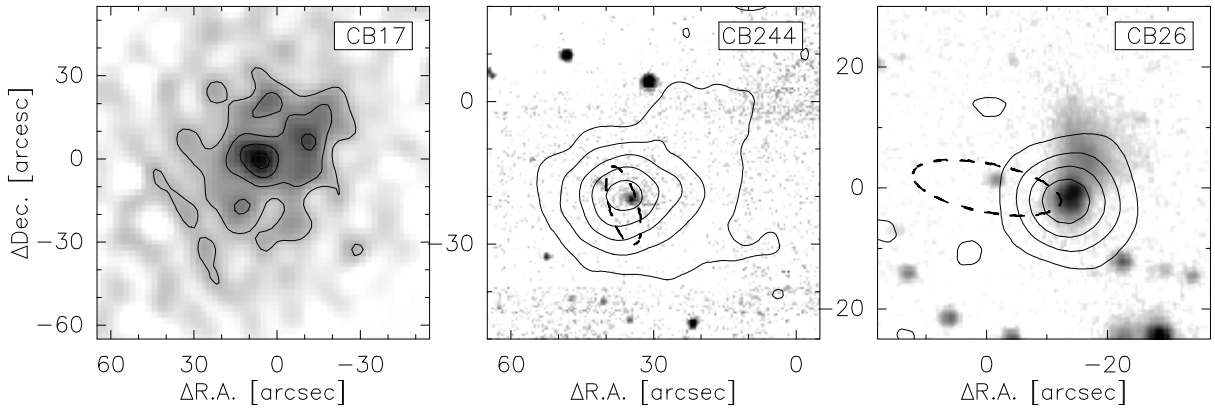

Figure 2: Millimeter dust continuum images of **a)** a pre-protostellar core (CB 17), **b)** a Class 0 protostellar core (CB 244, contours overlayed on a K-band image), and **d)** a disk-dominated Class I YSO (CB 26, contours overlayed on a K-band image; Launhardt & Sargent 2001). Dashed ellipses show IRAS point sources.

Figure 2a shows a 1.3 mm dust continuum map one such core (CB 17, Launhardt et al. in prep.). As this map shows and as already mentioned by Ward-Thompson et al. (1999), most pre-protostellar cores are far from being spherically symmetric; they typically have a rather filamentary structure and in some cases the flat inner cores seem to be fragmented. Evans et al. (2001) find that the large-scale morphology of many pre-protostellar cores can also be well-modeled by Bonnor-Ebert spheres with different degrees of central concentration, which could be an evolutionary effect. However, the filamentary structure and the turbulent nature of the outer envelopes (Falgarone et al. 1998; Park et al. 2004) make the assumption of an ideal Bonnor-Ebert gas sphere somewhat doubtful. For the same reason, radial density profiles should be taken with caution since models are usually fitted to circularly averaged emission profiles.

2.2 Class 0 protostellar cores

Isolated Class 0 protostellar cores have been observed in the submm/mm dust continuum emission and modeled by, e.g., Motte & André (2001), Shirley et al. (2002), and Launhardt et al. (in prep.). Molecular outflows have been mapped by, e.g., Yun & Clemens (1994). We have derived radial density profiles (and mean dust temperatures) for a number cores by fitting beam-convolved ray-traced core models to multi-wavelengths submm/mm dust emission maps (see Figs 3 and 4). The results compare well to those derived by other authors.

Isolated protostellar cores have a higher central mass concentration ($\frac{M_{5000\mathrm{AU}}}{M_{\mathrm{tot}}} \approx 0.4$) and appear to be more spherically symmetric than pre-protostellar cores. Their envelopes have a power-law radial density gradient of $n_{\mathrm{H}} \propto R^{-2\ldots-1.8}$ and a well-defined outer radius at $\sim 1\ldots2\times10^4$ AU. Densities inside $R < 3000-4000$ AU are up to more than two orders of magnitude higher than in pre-protostellar cores. Total masses are comparable to those of pre-protostellar cores, i.e., $2-5\,\mathrm{M}_\odot$. At their very center, higher dust temperatures and embedded accretion disks add additional dust emission, leading to strongly centrally peaked submm/mm continuum images. Envelope dust temperatures are comparable to those in pre-protostellar cores, which means that the embedded low-mass protostars usually do not considerably contribute much heating to the envelope. Although the average power-law index of the outer radial density profile resembles that of an isothermal sphere, no inner turn-over to shallower profiles ($p = 1.5$) could be confirmed in most sources, like predicted by the "standard" inside-out collapse model (Shu 1977). However, due to the limited angular resolution of most studies and the often unresolved and unknown contribution from an embedded accretion disk, this conclusion needs to be confirmed by detailed analysis of combined single-dish and interferometer data.

Cores in dense and clustered star-forming regions are expected to have different properties than isolated cores due to different environmental conditions like, e.g., better shielding from the external radiation field, differences in external pressure and turbulent environment, and effects of competitive accretion. Indeed, Johnstone et al. (2000) find smaller outer cutoff radii and smaller degrees of central condensation for cores in the ρ Ophiuchi molecular cloud.

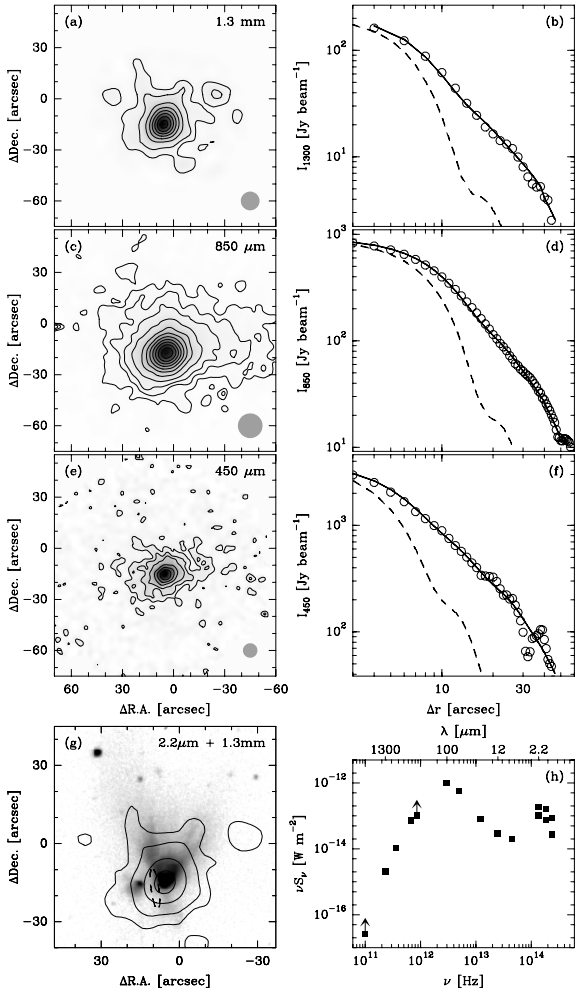

Figure 3: Submm/mm dust continuum maps and K-band image (lower left) of CB 230 (Class 0/I transition object). Observed and modeled radial emission profiles together with the beam profiles are shown in the right panels. SED at lower right. (Launhardt et al. in prep.)

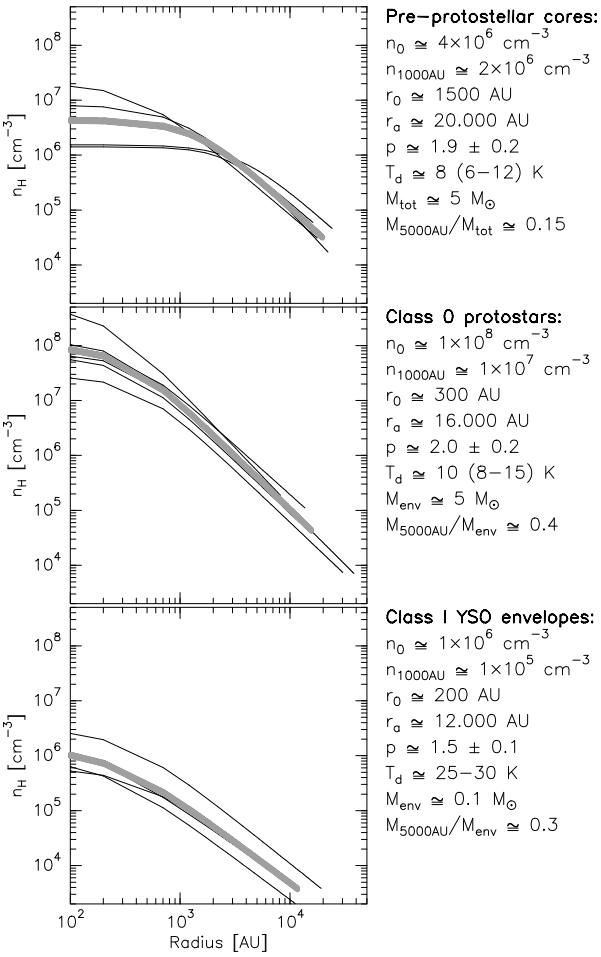

Figure 4: Radial density profiles of the form $n(r) = \frac{n_0}{\left(1+\frac{r}{r_0}\right)^p}$ for isolated pre-protostellar cores, Class 0 protostars, and Class I YSO envelopes, derived from model fits to the multi-wavelengths submm/mm dust emission maps. Thick grey curves show the averaged profiles. Central point sources in Class 0 and I (accretion disks) are not included. (Launhardt et al. in prep.)

2.3 Class I YSO envelopes

Class I sources are often also called "protostars", but we think of them rather as deeply embedded YSO's in an evolved, decelerated accretion stage with remnant envelopes. In contrast to Class 0 protostars, the mm continuum emission from the immediate circumstellar environment is dominated by an accretion disk rather than a dense infalling envelope. Systematic studies of the extended envelopes around Class I YSOs have been performed by, e.g., Young et al. (2003)

and Launhardt et al. (in prep.). The extended envelopes around isolated Class I YSOs have shallower density profiles ($p \approx 1.5$), lower densities ($n_{1000\mathrm{AU}} \approx 10^5\,\mathrm{cm}^{-3}$), higher dust temperatures (25–30 K), and much lower total masses ($\langle M_{\mathrm{env}} \rangle \approx 0.1\,\mathrm{M}_\odot$) than pre-protostellar and protostellar cores. Outer radii are about 10^4 AU. Depending on the viewing angle, the central star can be visible at NIR wavelengths, or the NIR emission is dominated by either scattered light from the outflow lobes or by shock-excited line emission from jets.

3 Multiplicity and efficiency of star formation

Although one would naively expect that simple isolated globules form one star each at their center, detailed studies in recent years showed that about 75% of star-forming cores in globules appear to be multiple on size scales between 500 AU (smallest observed scales) and 20000 AU (0.1 pc) (Launhardt 2003). This number includes true binary protostars (e.g., L 723 VLA 2, Launhardt et al. in prep.), embedded multiple YSOs (e.g., CB 230, Launhardt 2001), as well as multiple dense cores in a globule (e.g., CB 244) (see Fig. 5). While wide double cores like in CB 244 may not have formed by protostellar fragmentation nor may they lead to the formation of physical binary stars, high-resolution observations like for L 273, that would reveal binary protostars formed by fragmentation of a single protostellar core, do exist only for a handful of sources. This shows that even in isolated simple Bok globules star formation and fragmentation/multiplicity are inherently coupled, although exact numbers for the multiplicity rate cannot be given yet.

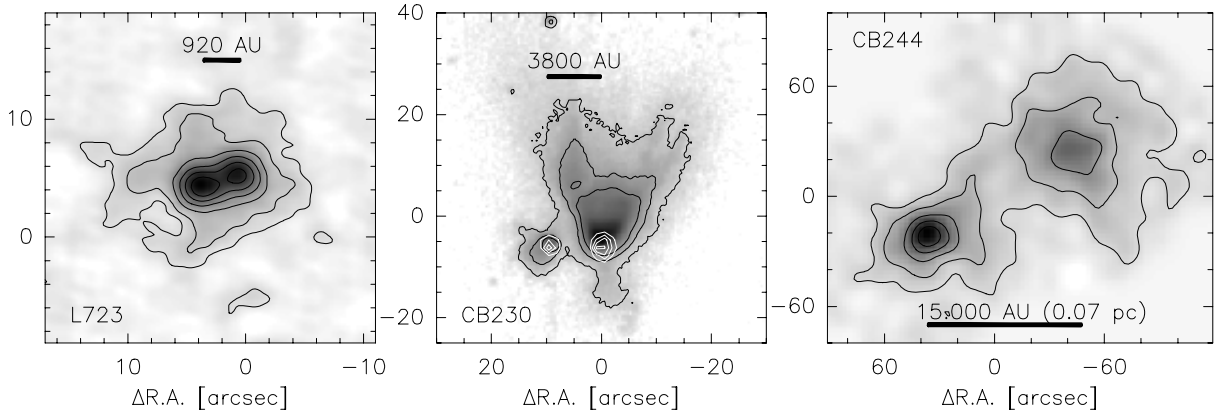

Figure 5: Isolated star formation and multiplicity: Left: 3 mm dust continuum image of L 723 VLA 2, showing a binary protostar with a projected separation of 920 AU. Middle: NIR image of CB 230 with 6.7 μm contours (white) superimposed, showing the two deeply embedded YSOs with a projected separation of $\sim$3800 AU. Right: 1.3 mm dust continuum image of the wide double core in the globule CB 244. The SE core is a Class 0 protostar, the NW core is of pre-protostellar nature.

It is often assumed that in the process of star formation, the mass of a clump or dense core is more or less completely transformed into stars. However, the average total mass in low-mass isolated pre-protostellar and protostellar cores ($R_{\mathrm{a}} \sim 1-2\times10^4$ AU) is about 5 $\mathrm{M}_\odot$. The typical mass within $R < 5000$ AU of a protostellar core (the assumed total size of the collapse region) is about 2 $\mathrm{M}_\odot$. The typical mass of stars that already have formed in globules is rather unknown. However, for the Class I YSO in CB 26, Launhardt & Sargent (2001) derive a mass of 0.3 $\mathrm{M}_\odot$ for the central star from the rotation curve of the circumstellar disk. Luminosities of stars with 12 μm IRAS PSC fluxes that are located within the projected boundaries of nearby Bok globules are typically 1–2 $\mathrm{L}_\odot$ (Launhardt 1996). Assuming an age of one to a few million years, this luminosity would indicate a stellar mass between 0.5 and 1 $\mathrm{M}_\odot$. Since these masses are also typical for stars formed in the isolated mode in the Taurus cloud, it is safe to assume that the

typical final stellar mass of a star or binary pair formed in an isolated low-mass core with the above properties is in the range $0.3-1\,M_\odot$. The efficiency whith which the mass of a cloud core is transformed into stellar mass would then be $6-20\%$ for the entire dense core ($R_a \sim 10^4$ AU) or $15-50\%$ of the mass included in the inner $R < 5000$ AU in a protostellar core.

4 Magnetic fields

Magnetic fields play a crucial role in star formation although it remains unclear at which stage (clump formation, fragmentation, protostellar collapse) and under which environmental conditions (isolated star formation vs. clustered mode in large and dense molecular clouds) turbulence or magnetic fields are the dominant force. Ward-Thompson et al. (2000), Henning et al. (2001), Wolf et al. (2003), and Crutcher et al. (2004) have obtained submillimeter dust emission polarization maps of a number of isolated prestellar and protostellar cores, i.e., of the dense and smooth inner cores, not the turbulent outer envelopes (see examples in Fig. 6). In most sources, the large-scale magnetic field structure appears to be well-ordered. By applying the Chandrasekhar-Fermi method, they estimate the mean magnetic field strengths in the plane of the sky for each source (dense cores only). Average magnetic field strength are $B \sim 125 \pm 40\,\mu$G in pre-protostellar cores and $\sim 170 \pm 50\,\mu$G in protostellar cores. Magnetic field strengths in the outer envelopes are much less-constrained. For the globule B 1, Goodman et al. (1989) measured $\sim 27\,\mu$G. Note however, that these are only order-of-magnitude estimates and the uncertainties are rather large.

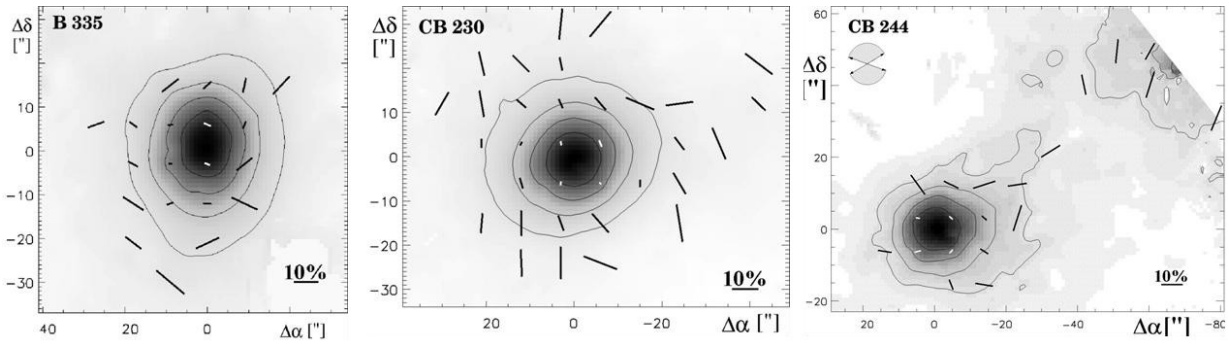

Figure 6: SCUBA images at 850 μm of B 335, CB 230, and CB 244, with polarization vectors superimposed. The polarization maps are used to derive the strengths and mean direction of the magnetic fields in these protostellar cores (from Wolf et al. 2003).

5 Distribution and evolution of angular momentum

Bok globules, like all celestial objects, have non-zero angular momentum and rotate. However, other sources of stochastic and systematic motion like, e.g., turbulence on different size scales, outflows, infall, and shearing can complicate the interpretation of velocity fields derived from molecular emission lines. Goodman et al. (1993) and Kane & Clemens (1997) have analyzed velocity fields and rotation curves of Bok globules and isolated cores in Taurus. They find that most clouds / cloud cores are rotating in approximate solid-body motion with specific angular momenta scaling with cloud size (i.e., approximate conservation of angular velocity) and being consideralby larger than that of T Tauri binary systems. However, stars do not form from the entire cloud, but only from the dense inner $R \approx 5000$ AU part of the cores that undergoes dynamical gravitational collapse and decouples from the rest of the cloud. Detailed kinematic studies of pre-protostellar cores (e.g., IRAM04191, Belloche et al. 2002; CB 17, Launhardt et al. in prep.) and binary protostellar cores (e.g., CB 230, Launhardt 2001, 2003, see Fig. 7) show

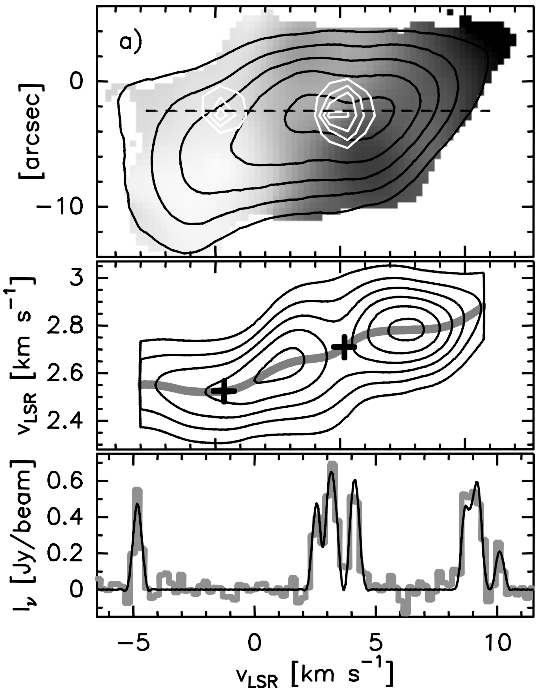

Figure 7: Kinematic structure of the protostellar double core in CB 230. Top: integrated N_2H^+ map (black contours) and mean velocity map (grey-scale, white to black: 2.4 to 2.9 km s^{-1}). White contours show the embedded MIR sources observed with ISOCAM. Center: position-velocity diagram along the dashed line in top panel. Bottom: N_2H^+(1–0) spectrum and fit (Launhardt 2000).

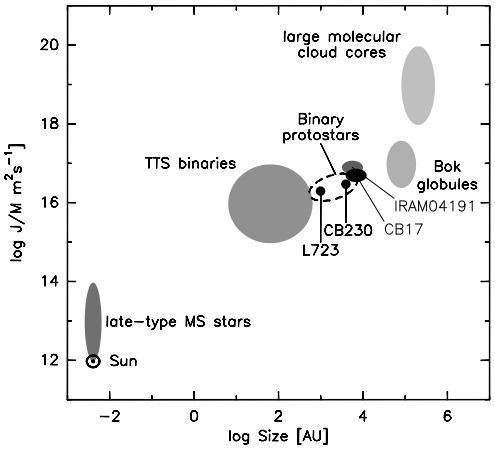

Figure 8: Specific angular momentum vs. size scale for different astronomical sources, from large molecular cloud cores to MS stars. CB 17 (Launhardt et al. in prep) and IRAM 04191 (Belloche & André 2004) are pre-protostellar cores. Binary protostars from Launhardt (2003).

that on size scales below $R \approx 5000$ AU, angular momenta do not scale (or scale only weakly) with size (i.e., angular momentum is conserved). The (specific) angular momentum of prestellar and protostellar cores on these size scales is comparable or only a factor of few larger than that of typical T Tauri binary systems (see Fig. 8). In the context that most protostellar cores are assumed to fragment and form binary stars, this means that most of the angular momentum contained in the collapse region is transormed into orbital angular momentum of the resulting stellar binary system.

6 Energy balance

Here, we attempt to estimate the contribution of different terms to the total energy balance of "typical" (average) isolated low-mass pre-protosteller and protostellar cores. Table 2 summarizes the basic (simplified) equations and the estimated numbers for the thermal, turbulent, rotational kinetic, magnetic, and gravitational potential energy content for the inner 5000 AU and the entire source of both pre-protostellar and protostellar cores. We assume average total gass masses and temperatures listed in Table 2 and radial density profiles of $\rho \propto R^{-1}$ in the inner 5000 AU of pre-protosteller cores and $\rho \propto R^{-2}$ everywhere else.

At the given temperatures, thermal FWHM line widths for a mean particle of mass $2.33 \times m_{\rm H}$ are in the range $\Delta v_{\rm therm} = \sqrt{8 \ln 2} \sqrt{\frac{kT}{2.33\, m_{\rm H}}} = 0.4 - 0.5\,{\rm km\,s^{-1}}$. Observed FWHM widths of optically thin N_2H^+ and NH_3 lines (tracing dense gas in the cores) towards isolated pre-protostellar and protostellar cores (where not strongly affected by outflow or systematic infall motions) are in the range $0.35 - 0.4\,{\rm km\,s^{-1}}$ (e.g., Benson & Myers 1989; Benson et al. 1998).

Table 2: Energy balance of globule cores

Term	Equation[a]	Pre-protostellar		Class 0	
		$R \leq 5000\,\mathrm{AU}$ ($M = 1\,\mathrm{M}_\odot$) ($T = 8\,\mathrm{K}$)	$R \leq 20000\,\mathrm{AU}$ ($M = 5\,\mathrm{M}_\odot$) ($T = 12\,\mathrm{K}$)	$R \leq 5000\,\mathrm{AU}$ ($M = 2\,\mathrm{M}_\odot$) ($T = 10\,\mathrm{K}$)	$R \leq 16000\,\mathrm{AU}$ ($M = 5\,\mathrm{M}_\odot$) ($T = 12\,\mathrm{K}$)
E_therm	$\frac{3}{2}\,M\,\frac{k\,T}{\mu\,m_\mathrm{H}}$	4×10^{34} J	3×10^{35} J	1×10^{35} J	3×10^{35} J
E_turb	$\frac{3}{2}\,M\,\langle v_\mathrm{x}^2 \rangle$	2×10^{34} J	3×10^{35} J	6×10^{34} J	4×10^{35} J
E_rot	$\frac{\alpha_\mathrm{rot}}{2}\,M\,R^2\,\omega^2$ [b]	1.5×10^{33} J	2.5×10^{33} J	2×10^{34} J	3×10^{34} J
E_mag	$\frac{1}{6}\,R^3\,B^2$	1×10^{35} J	4×10^{35} J	2×10^{35} J	4×10^{35} J
$-E_\mathrm{grav}$	$\alpha_\mathrm{vir}\,M^2\,R^{-1}\,G$ [c]	2.4×10^{35} J	2×10^{36} J	1.4×10^{36} J	2.8×10^{36} J

[a] Approximation for an ideal gas sphere of radius R, mass M, and temperature T. Furthermore, $\mu = 2.33$ is the mean molecular weight, m_H is the mass of an hydrogen atom, k is the Boltzman constant, $\langle v_\mathrm{x}^2 \rangle$ is the mean quadratic one-dimensional turbulent velocity dispersion of the gas (related to the FWHM line width by $\sqrt{\langle v_\mathrm{x}^2 \rangle} = \frac{\Delta v_\mathrm{turb}}{\sqrt{8\,\ln 2}}$), ω is the rotational angular velocity of the cloud core (assuming solid-body rotation), B is the average magnetic field strength, and G is the gravitational constant.
[b] $\alpha_\mathrm{rot} = \frac{2}{5+2\,p}$, where p is the radial density power-law index (see Fig. 4). [c] $\alpha_\mathrm{vir} = \frac{3-p}{5-2\,p}$.

Fuller & Myers (1992) and others report mean $C^{18}O$ line widths tracing core and envelope) of $0.4-0.5\,\mathrm{km\,s^{-1}}$ for starless cores and $0.5-0.7\,\mathrm{km\,s^{-1}}$ for protostellar cores. Neglecting possible contributions from systematic mass motions, turbulent contributions to FWHM line widths are then $\Delta v_\mathrm{NT} \approx 0.35\,\mathrm{km\,s^{-1}}$ for the inner 5000 AU in both pre-protostellar and protostellar cores and $\approx 0.4 - 0.6\,\mathrm{km\,s^{-1}}$ in the outer envelopes.

The numbers for the thermal and turbulent energy content calculated from these estimates show that in the inner 5000 AU of both pre-protostellar and protostellar cores thermal contributions slightly outweight turbulence, while in the outer envelopes turbulence appears to dominate (see Table 2). This is consistent with Falgarone et al. (1998), Park et al. (2004), and others who find that the outer envelopes of starless cores are clumpy and turbulent, while the inner cores appear to be more quiet and smooth with a power-law density distribution. Rotational kinetic energies derived from measured rotation curves (see Sect. 5) appear to be much lower than thermal and turbulent contributions. The magnetic energy content derived from measured magnetic field strengths (Sect. 4) appears to be larger than the other contributions, implying that magnetic fields play an important role in supporting the dense cores against gravitational collapse or at least delaying the collpase. However, the uncertainties in magnetic field strength and mean core radius are rather large and the dependence is strongly non-linear, so that this statement should be taken with caution.

When we apply the equilibrium viral theorem $2\,[E_\mathrm{th} + E_\mathrm{turb} + E_\mathrm{rot}] + E_\mathrm{mag} + E_\mathrm{grav} = 0$, we find that pre-protostellar cores are close to virial equilibrium, while Class 0 protostellar cores (in particular the inner 5000 AU) are significantly supercritical (by a factor of $2 - 2.5$).

7 Summary

Dense cores of nearby isolated Bok globules are ideal laboratories to study in detail the process of low-mass star formation. However, one has to keep in mind that some of the results may be typical only for the isolated mode of star formation and may not be directly applicable to dense and clustered star-forming regions. The main results can be summarized as follows:

1. Many Bok globules with typical total gas masses $5 - 50\,\mathrm{M}_\odot$ and sizes $0.1 - 1\,\mathrm{pc}$ contain dense cores and form stars of typical mass $0.3 - 1\,\mathrm{M}_\odot$. The dense cores typically contain $10 - 20\%$ of the total mass in the globule and have sizes of $10000 - 20000\,\mathrm{AU}$. It is still under debate if smaller globules with less-prominent cores can form lower-mass stars or even substellar objects.

2. Most globules are slightly cometary or irregularly shaped and have the dense core located closer to the sharper rim ("head" side).

3. Pre-protostellar cores often appear filamentary and have very irregular and relatively turbulent outer envelopes. Mean radial density profiles in the inner few thousand AU are rather flat and approach R^{-2} further out.

4. Class 0 protostellar cores have a higher central mass concentration and appear to be more spherically symmetric than pre-protostellar cores. Their envelopes have a power-law radial density gradient of $n_\mathrm{H} \propto R^{-2}$ and a well-defined outer radius at $\sim 1.5 \times 10^4\,\mathrm{AU}$. Most observations have not found a turn-over to shallower density profiles in the inner expected collapse region.

5. Most star-forming cores in globules appear to be multiple on size scales between 500 AU and 20000 AU. While some globules contain initially separate dense cores that collapse and evolve independently, many cores appear to fragment in the process of protostellar collapse and form binary or multiple stellar systems.

6. The (specific) angular momentum contained in the inner $\approx 5000\,\mathrm{AU}$ of isolated protostellar cores is comparable or only a factor of few larger than that of typical T Tauri binary systems, i.e. most of the angular momentum contained in the collapse region is transormed into orbital angular momentum of the resulting stellar binary systems.

7. Only about $6-20\%$ of the mass of a dense core ($R < 20000\,\mathrm{AU}$) is transformed into stars. For the inner $R < 5000\,\mathrm{AU}$ of protostellar cores, this efficiency goes up to $15-50\%$.

8. Typical magnetic field strength are $B \sim 125\,\mu\mathrm{G}$ in pre-protostellar cores, $\sim 170\,\mu\mathrm{G}$ in protostellar cores, and $\sim 30\,\mu\mathrm{G}$ in the outer envelopes. However, the uncertailnties are rather large.

9. Although numbers for the magnetic field strengths are somewhat uncertain, the main support against gravitational collapse of the dense inner cores appears to come from magnetic fields, followed by thermal pressure. Only in the outer envelopes turbulent support becomes equally important. Rotational kinetic energies are about one order of magnitude lower than other contributions. Pre-protostellar cores are close to virial equilibrium, while Class 0 protostellar cores (in particular the inner 5000 AU) are significantly supercritical.

Acknowledgments

I wish to thank Th. Henning, T. Khanzadyan, S. Wolf, D. Ward-Thompson, R. Zylka, T. Bourke, A. Sargent, H. Zinnecker, Y. Pavluchenkov, and L. V. Tóth who all contributetd in one way or the other to the work on which this review is based. I also want to thank P. André, A. Burkert, and M. Smith for helpful discussions.

References

1. Belloche, A., André, P., Despois, D., & Blinder, S. 2002, A&A, 393, 927
2. Benson, P. J. & Myers, P. C. 1989, ApJS, 71, 89
3. Benson, P. J., Caselli, P., & Myers, P. C. 1998, ApJ, 506, 743
4. Bourke, T. L., Hyland, A. R., & Robinson, G. 1995, MNRAS, 276, 1052 (BHR)
5. Clemens, D. P. & Barvainis, R. 1988, ApJS, 68, 257 (CB)
6. Crutcher, R. M., Nutter, D. J., Ward-Thompson, D., & Kirk, J. M. 2004, ApJ, 600, 279
7. Evans, N. J., Rawlings, J. M. C., Shirley, Y. L., & Mundy, L. G. 2001, ApJ, 557, 193
8. Falgarone, E., Panis, J.-F., Heithausen, A., Perault, M., Stutzki, J., Puget, J.-L., & Bensch, F. 1998, A&A, 331, 669
9. Fuller, G. A. & Myers, P. C. 1992, ApJ, 384, 523
10. Goodman, A. A., Crutcher, R. M., Heiles, C., Myers, P. C., & Troland, T. H. 1989, ApJ, 338, L61
11. Goodman, A. A., Benson, P. J., Fuller, G. A., & Myers, P. C. 1993, ApJ, 406, 528
12. Johnstone, D., Wilson, C. D., Moriarty-Schieven, G., Joncas, G., Smith, G., Gregersen, E., & Fich, M. 2000, ApJ, 545, 327
13. Henning, T., Wolf, S., Launhardt, R., & Waters, R. 2001, ApJ, 561, 871
14. Kane, B. D. & Clemens, D. P. 1997, AJ, 113, 1799
15. Launhardt, R. 1996, Ph.D. Thesis, University of Jena
16. Launhardt, R. 2001, IAU Symposium, 200, 117
17. Launhardt, R. 2003, IAU Symposium, 221, 140
18. Launhardt, R. & Sargent, A. I. 2001, ApJ, 562, L173
19. Motte, F. & André, P. 2001, A&A, 365, 440
20. Park, Y., Lee, C. W., & Myers, P. C. 2004, ApJS, 152, 81
21. Shirley, Y. L., Evans, N. J., & Rawlings, J. M. C. 2002, ApJ, 575, 337
22. Shu, F. H. 1977, ApJ, 214, 488
23. Ward-Thompson, D., Scott, P. F., Hills, R. E., & André, P. 1994, MNRAS, 268, 276
24. Ward-Thompson, D., Motte, F., & André, P. 1999, MNRAS, 305, 143
25. Ward-Thompson, D., Kirk, J. M., Crutcher, R. M., Greaves, J. S., Holland, W. S., & André, P. 2000, ApJ, 537, L135
26. Wolf, S., Launhardt, R., & Henning, T. 2003, ApJ, 592, 233
27. Young, C. H., Shirley, Y. L., Evans, N. J., & Rawlings, J. M. C. 2003, ApJS, 145, 111
28. Yun, J. L. & Clemens, D. P. 1994, ApJS, 92, 145